

**POWER GENERATION WITH VORTEX INDUCED
VIBRATIONS**

A Final Year Project Report

Presented to

SCHOOL OF MECHANICAL & MANUFACTURING ENGINEERING

Department of Mechanical Engineering

NUST

ISLAMABAD, PAKISTAN

In Partial Fulfilment

of the Requirements for the Degree of
Bachelor of Mechanical Engineering

by

Muhammad Shahzaib Asim

Hafiz Muhammad Osama Khan

Hassan Majeed Akhund

Muhammad Abdullah Hassan Malik

June 2022

EXAMINATION COMMITTEE

We hereby recommend that the final year project report prepared under our supervision by:

MUHAMMAD SHAHZAIB ASIM	253190
HAFIZ MUHAMMAD OSAMA KHAN	256676
HASSAN MAJEED AKHUND	260508
MUHAMMAD ABDULLAH HASSAN MALIK	261476

Titled: "POWER GENERATION WITH VORTEX INDUCED VIBRATIONS" be accepted in partial fulfilment of the requirements for the award of BACHELOR'S IN MECHANICAL ENGINEERING degree with grade ____

Supervisor: Dr Adnan Munir, Prof. Supervisor	Dated: _____
Committee Member: Name, Title (faculty rank) Affiliation	Dated: _____
Committee Member: Name, Title (faculty rank) Affiliation	Dated: _____

(Head of Department)

(Date)

COUNTERSIGNED

Dated: _____

(Dean / Principal)

ABSTRACT

The focus of the project is to develop a clean green source of energy production by utilising the renewable kinetic energy of a flowing body of water by incorporating a cylindrical structure that oscillates in the flow regime by naturally occurring vortices in its wake.

The working phenomenon behind the oscillation is vortex shedding that asserts lift and drag forces on the cylindrical structure due to which the cylinder vibrates. A secondary stationary cylinder is used in tandem to amplify the vibrations by utilising the phenomenon of wake induced vibration. By attaching a generator-based electricity generation system to the oscillating body, we can harvest the kinetic energy and convert it into electrical energy.

ACKNOWLEDGMENTS

We would like to thank Allah Almighty first and foremost for all the help that He has provided us, to thank our parents for their prayers and guidance, and Dr Adnan Munir for his patience and support.

ORIGINALITY REPORT

PaperPass .net

Title Power Generation With Vortex Induced Vibrations

9% SIMILARITY INDEX
Date: 2022-05-29 19:09:55(+00:00 UTC)
Report ID: 6293c50776c0200b
Word count: 4902
Character count: 25100

9% ACADEMIC
0% INTERNET

11	• Predicting vortex-induced vibration from driven oscillation results • J.S. Leonini, B.E. Stewart, M.C. Thompson, K. Hourigan • Applied Mathematical Modelling, 2008 Academic	0.3%
12	• Numerical study for vortex induced vibration of a circular cylinder in high-Reynolds-number flow • KAZUHIRO TSUBOKI, TETSURO TAMURA, KUNIO KIJUWAHARA • 27th Aerospace Sciences Meeting, 1989 Others	0.3%
13	• Riser Design • William Thomas • Encyclopedia of Maritime and Offshore Engineering, 2018 Others	0.3%
14	• Alternative energy using vortex-induced vibration from turbulent flows: theoretical and analytical analysis • M.A. Zahedi, S.S. Dal • 5th Biennial International Conference on Engineering and Technology (BICET 2014), 2014 Others	0.3%
15	• Transition scenario of a sphere freely falling in a vertical tube • Thibaut Delisle, Yannick Heesari, Jérôme Dufek • Journal of Fluid Mechanics, 2012 Academic	0.3%
16	• The vortex shedding around four circular cylinders in an in-line square configuration • Fellei, Tong-Liang, Cheng-Ming, Zhao, Tongming, Zhou, Xiao-bo, Chen • Physics of Fluids, 2014 Academic	0.3%
17	• Numerical analysis of vortex-induced motion of two-dimensional circular cylinder by finite Boltzmann method • Shinobu Hirabayashi • Journal of Marine Science and Technology, 2016 Academic	0.3%
18	• On the applicability of the Forchheimer equation in simulating flow through woven screens • Meir Taler • Biocystems Engineering, 2011 Academic	0.3%
19	• The effect of base column on vortex-induced vibration of a circular cylinder with low aspect ratio • Yuanchuan Liu, Fushun Liu, Enhao Wang, Qing Xiao, Liang Li • Ocean Engineering, 2020 Academic	0.3%
20	• The effect of inclination on vortex-induced vibration of a circular cylinder with a base column • Yuanchuan Liu, Fushun Liu, Qing Xiao, Lin Zhou • Ocean Engineering, 2020 Academic	0.3%

Similar sources		
• Vortex Induced Vibration of Circular Cylinder With Two Degrees of Freedom: Computational Fluid Dynamics vs. Reduced-Order Models • Wang, Qing, Xiao, Nanakorn, Sritul, Hossain, Zanganeh-Order Models • Volume 7: CFD and VIV, 2013 Others		0.4%
1	• Dynamics vs. Reduced-Order Models • Wang, Qing, Xiao, Nanakorn, Sritul, Hossain, Zanganeh-Order Models • Volume 7: CFD and VIV, 2013 Others	0.4%
2	• Flow past a rotating circular cylinder with superhydrophobic surfaces • Ren, Y., Li, Xiong, D., Yang, J., Duan • Acta Mechanica, 2018 Academic	0.4%
3	• Suspension flow past a cylinder: particle interactions with recirculating wakes • Hamed Haadadi, Shahab Shojaei-Zadeh, Kevin Conington, Jeffrey F. Morris • Journal of Fluid Mechanics, 2014 Academic	0.4%
4	• Laminar vortex shedding behind a cooled circular cylinder • Zhenliang Tai, Mingliang An, Bang Wang, Wen-Yun Tu • Experiments in Fluids, 2014 Academic	0.4%
5	• Sports Ball Aerodynamics • Roberto D. Maitte • Sport Aerodynamics CISM International Centre for Mechanical Sciences, 2008 Others	0.4%
6	• Flow past an oscillating circular cylinder in a channel with an upstream splitter plate • Bayram Cank, Ulkar Hiding, Sibel Guner, Ali Baskak • Physics of Fluids, 2008 Academic	0.4%
7	• Hydrometallurgical Processes • Milton E. Wallworth, Jan D. Miller • Rate Processes of Extractive Metallurgy, 1979 Others	0.4%
8	• Flow separation in the inlet valve gap of piston engines • M. Wiedas, A. Melting, F. Duntz • Progress in Energy and Combustion Science, 1998 Academic	0.4%
9	• Direct and Large-EDR/OPTAC Series 2001-Entry Simulation IV • Others	0.4%
10	• Re-examination of laminar flow over twin circular cylinders in tandem arrangement • Ming-Ming Liu, Lin Lu, Bin Tang, Ming Zhao, Guo-Qiang Tang • Fluid Dynamics Research, 2014 Academic	0.3%
21	• Numerical simulation of vortex-induced vibration of a circular cylinder at low mass-damping ratio • RANG COOZ Y., PAN, W. C., CHU, G. M., MAO • Journal of Fluids and Structures, 2007 Academic	0.2%
22	• A Wake Oscillator With Frequency-Dependent Tuning Coefficients for the Modeling of VIV • H. M. Dyrh, A. V. Melnikin • Volume 5: Materials Technology: CFD and VIV, 2008 Others	0.2%
23	• Three-dimensional numerical investigation of vortex-induced vibration of a rotating circular cylinder in uniform flow • Adrian Kunz, Ming Zhao, Helen Wu, Lin Lu, Dazhi Ning • Physics of Fluids, 2016 Academic	0.2%
24	• The Experimental Study of Vortex-Induced Vibration of Submarine Pipelines in Steady Current • Guchun Wang • ICPTT 2009, 2009 Academic	0.2%
25	• A prediction technique for the transient vortex-induced oscillations of tensioned risers • G. Bontempi, A. Campaniti • Ocean Engineering, 2002 Academic	0.2%
26	• An experimental investigation of free-induced vibration of high-rise-ratio rectangular cylinders • Jinhong Zhao, Kang Houqian, Mark C. Thompson • Journal of Fluids and Structures, 2019 Academic	0.2%
27	• A novel reduced order model for vortex induced vibrations of long flexible cylinders • Giovanni Stallo, Hans-Joerg D. Matthies, Claudio Borri • Ocean Engineering, 2018 Academic	0.2%
28	• Large Eddy Simulation of Fluid Elastic Instability in Square Normal Cylinder Array • Vasil Strelac, Elizabeth Longtin, Franck Bai • Volume 5: High-Pressure Technology: Rudy Sumanuzzo Student Paper Competition and 23rd Annual Student Paper Competition: ASME NDE Division, 2016 Others	0.2%
29	• Numerical simulation of unsteady flow patterns around a vibrating circular cylinder • TETSURO TAMURA, KAZUHIRO TSUBOKI, KUNIO KIJUWAHARA • 26th Aerospace Sciences Meeting, 1988 Others	0.2%
30	• On computations of temperature-dependent incompressible flows by high-order methods • Jun Park • EPJ Web of Conferences, 2016 Academic	0.2%
31	• Vortex Shedding - an overview ScienceDirect Topics • https://www.sciencedirect.com/topics/engineering/vortex-shedding?via=ihub&query=VIV%20cylinder%20shedding&work%3Dour%20data%20set%20number	0.1%

TABLE OF CONTENTS

ABSTRACT.....	ii
ACKNOWLEDGMENTS	iii
ORIGINALITY REPORT	iv
TABLE OF CONTENTS.....	v
LIST OF FIGURES	vii
LIST OF TABLES	x
ABBREVIATIONS	xi
NOMENCLATURE	xi
CHAPTER 1: INTRODUCTION.....	1
1.1 Problem Statement	2
1.2 Motivation	2
CHAPTER 2: LITERATURE REVIEW	3
2.1 Vortex Shedding and Vortex Induced Vibrations	3
2.2 The Lock-in Region	4
2.3 Cylinders in Tandem	5
2.4 Power Generation	6
2.5 Existing Work	8
CHAPTER 3: METHODOLOGY	10
3.1 Process Summary	10

3.2	Numerical Model.....	11
3.3	Flow Domain.....	13
3.4	Prototype Design.....	18
3.4.1	Design Specification.....	18
3.4.2	Final design.....	20
CHAPTER 4: RESULTS AND DISCUSSION.....		26
4.1	Numerical Study Result for Single Cylinder.....	26
4.2	Numerical Simulation for Cylinders in Tandem.....	27
4.3	Displacement Results for Prototype.....	29
4.4	Power Generation Results.....	31
CHAPTER 5: CONCLUSION AND RECOMMENDATION.....		33
APPENDIX I: TIME HISTORY GRAPHS OF DISPLACEMENT OF SINGLE CYLINDER.....		34
APPENDIX II: TIME HISTORY GRAPHS OF DISPLACEMENT OF TANDEM CYLINDERS.....		37
APPENDIX III: DRAWINGS OF COMPONENTS.....		42
REFERENCES.....		46

LIST OF FIGURES

Figure 1: Illustration of Lock in in Water, Tørum & Anand (1985).....	5
Figure 2: The model of Lefebure et. al., utilising a belt	7
Figure 3: Electromagnetic generation set up from Soti et. al	9
Figure 4: VIVACE Module	9
Figure 5: Process Flowchart.....	10
Figure 6: Full flow domain	14
Figure 7: Inflation layer	14
Figure 8: Near field triangular and far field quad mesh.....	14
Figure 9: Mesh of the flow field for Cylinders in Tandem.....	15
Figure 10: Mesh around the cylinders	15
Figure 11: Close up of the tandem mesh	16
Figure 12: Contour plot of Y+ value.....	17
Figure 13: Initial Design	19
Figure 14: Final Design	20
Figure 15: Linear slide rail schematic.....	23
Figure 16: Energy Extraction Mechanism	24
Figure 17: Amplitude vs Reduced Velocity for a Single Cylinder. Literature (top) vs. Current Results (bottom).....	26
Figure 18: Oscillation magnitude vs Reduced Velocity, Assi et. Al. (top) and current results (bottom)	28

Figure 19: Practical Results of Oscillation Magnitude vs Flow Speed	30
Figure 20: Practical results In terms of Reduced Velocity	30
Figure 21: Displacement time history at $V_r 2$	34
Figure 22: Displacement time history at $V_r 3$	34
Figure 23: Displacement time history at $V_r 4$	34
Figure 24: Displacement time history at $V_r 5$	35
Figure 25: Displacement time history at $V_r 6$	35
Figure 26: Displacement time history at $V_r 7$	35
Figure 27: Displacement time history at $V_r 8$	36
Figure 28: Displacement Time History at $V_r 2$ and in between distance $1.5D$	37
Figure 29: Displacement Time History at $V_r 4$ and in between distance $1.5D$	37
Figure 30: Displacement Time History at $V_r 6$ and in between distance $1.5D$	38
Figure 31: Displacement Time History at $V_r 8$ and in between distance $1.5D$	38
Figure 32: Displacement Time History at $V_r 2$ and in between distance $2D$	39
Figure 33: Displacement Time History at $V_r 4$ and in between distance $2D$	39
Figure 34: Displacement Time History at $V_r 2$ and in between distance $3D$	40
Figure 35: Displacement Time History at $V_r 4$ and in between distance $3D$	40
Figure 36: Displacement Time History at $V_r 6$ and $V_r 8$ and in between distance $3D$	41
Figure 37: Drawing of Rack	42
Figure 38: Drawing of Motor Holders	42

Figure 39: Drawing of Pipe Bracket43

Figure 40: Drawing of Top Plate43

Figure 41: Drawing of Motor Gear44

LIST OF TABLES

Table 1: Results of grid dependence study	17
Table 2: Amplitude of Oscillation at different reduced velocities and distances between cylinders.....	27
Table 3: Amplitude of Oscillation at different flow speeds and distances between cylinders	29
Table 4: Electric Reading Results	32

ABBREVIATIONS

VIVs Vortex Induced Vibrations

NOMENCLATURE

V_R Reduced Velocity

D Diameter of Cylinder

ν Kinematic Viscosity

Re Reynolds Number

f_n Natural Frequency

CHAPTER 1: INTRODUCTION

In the world of power generation, humanity was much too concerned with the production of useful electrical energy using non-renewable fuel however in the modern age we see the negative effects of such use in the form of pollution, climate change and imminent catastrophe if we do not find alternative source of energy generation.

That is where renewable natural energy sources come into play and when we use these sources, we can completely nip pollution in the bud and save our world while providing the much-needed energy to serve humanity.

One such source of energy is the kinetic energy of a flow regime in every river, ocean or body of water and harvesting that energy is the focus of our project.

It is commonly observed that when a cylindrical structure such as a pipe or cable is submerged in a flow regime then around that structure, vortices are produced simply due to the flow.

These vortices are also observed to “oscillate” between upward and downward vortex such that when the downward vortex is dying, it gives rise to an upward vortex. Similarly, downward vortices are also produced when the upward vortices die.

During the lifetime of a vortex, it applies a force to the cylindrical structure in the form of lift and drag.

As mentioned, the vortices oscillate between upward and downward vortex, so obviously the applied force will also oscillate at a frequency defined by a dimensionless parameter known as ‘Strouhal Number’

$$St = \frac{f_{st}D}{U}$$

where f_{st} is the vortex shedding frequency.

Therefore, the applied force by the vortices will also oscillate and due to these force oscillations, the cylindrical structure will vibrate.

The aim of our FYP is to utilize these naturally occurring vibrations into consumable power.

1.1 Problem Statement

To generate electricity from the vortex induced vibrations on a cylindrical structure when exposed to a turbulent flow regime.

1.2 Motivation

The world is accustomed to the consumption of electrical energy in every single aspect of our lives, so it is no question that production of electrical energy is of the utmost importance to every human living in this world.

This need for electrical energy demanded the consumption of non-renewable fuel sources that fulfilled the need, albeit at a cost to the environment. Pollution and climate change has shown their devastating effect at an extremely alarming pace due to which the world has recognized the need to shift to clean and renewable energy sources such as wind, solar and tidal energy.

Respecting this need is the motivation behind the project as it will utilize the renewable kinetic energy of a flow regime in any body of water to produce clean and safe energy.

CHAPTER 2: LITERATURE REVIEW

In the last few decades, research has begun to pick up into ways of utilising the energy that could be produced using vortex induced motion. Many differing methods have been suggested and one of them is the use of Vortex Induced Vibrations (VIVs). Several analyses have been performed, both and using Computational Fluid Dynamics (CFD) simulations. Most of the work undertaken has been into exploring the phenomenon of VIVs, and the several factors that affect it, especially the non-dimensional reduced velocity, V_r . The generation of power with VIVs is a relatively new field.

2.1 Vortex Shedding and Vortex Induced Vibrations

For a body present in fluid flow, it is well known that the flow will exhibit the creation of vortices in the wake of the body. Furthermore, it is known that for a circular body placed in steady flow, vortex shedding begins to occur at Reynolds numbers greater than 47 (Williamson & Roshko, 1988). Reynold's Number is defined as $Re = UD/\nu$, where U is the fluid velocity, D would be the cylinder diameter, and ν is the fluid's kinematic viscosity. Observations and experiments show that the wake of a bluff body will comprise a vortex street, which is created due to the periodic separation of flow at the boundary layer. The vortices on one side grow, are stretched out, and then shed, after which this process repeats for the other side. The shape and type of vortex shedding will then depend on the magnitude of the Reynolds numbers and the geometric properties of the body. The frequency of vortex shedding can be represented by the Strouhal number, a constant value that evaluate to the ratio fD/U , where f is the

frequency of vortex shedding. The Strouhal number for a smooth cylinder evaluates to about 0.20 (Sarpkaya, 1979).

It is now well documented (Sarpkaya, 1979) that when the vortex shedding frequency begins to approach the natural frequency of the cylinder, the Strouhal relationship is overwritten and the frequency of vortex shedding, and body oscillation become the same. At this point, the vortices began to induce a larger vibration in the cylinder itself. This phenomenon is called lock-in.

2.2 The Lock-in Region

If a cylinder is mounted elastically in oncoming steady flow, and the frequency of vortex shedding matches the natural frequency of the cylinder, a large amplitude vibration is produced within the cylinder. This phenomenon is called the 'lock-in', as first explored by Bishop & Hassan in 1964 and further by Govardhan & Williamson in 2000. It has been observed that the lock-in region depends mainly on the reduced velocity of the flow, occurring mainly within a specific range. Reduced velocity, V_r , is a non-dimensional parameter defined as $V_r = U/(f_n D)$, where f_n is the natural frequency of the cylinder.

Normally, the frequency of vibration follows the frequency of vortex shedding, which is illustrated by the Strouhal law. However, within lock-in, the frequency of vibration deviates from this relationship and becomes almost constant, 'locking in' to that frequency. The phenomenon was explored extensively by several researchers including Feng (1968) and Tørum & Anand (1985) in air and water, respectively. The lock-in range occurs in the vicinity of a reduced velocity of 2-10, depending on factors such as the mass of the cylinder, turbulence and surface roughness.

The increase in amplitude of vibration during the lock-in region is significant enough to consider the utilisation of the energy into the generation of electricity.

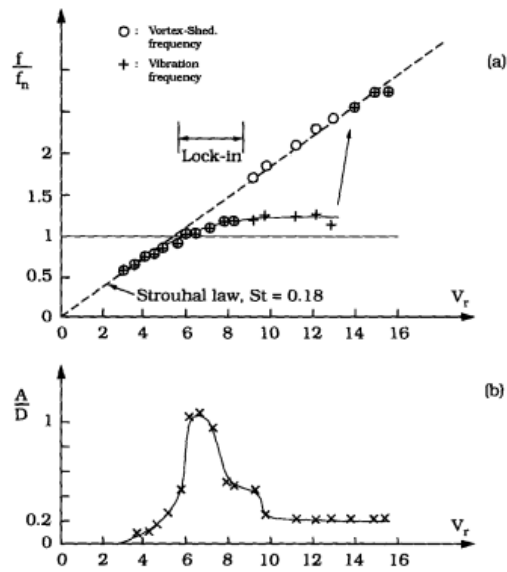


Figure 1: Illustration of Lock in in Water, Tørum & Anand (1985)

2.3 Cylinders in Tandem

Considering that the main concern is the increase of the amplitude of vibration, the effect of using cylinders in tandem can be considered. In 2006, Assi et al. showed that for a trailing free cylinder oscillating in the wake of a fixed leading one, the amplitude of the vibration of the fixed cylinder can exceed that of a single cylinder under similar conditions. The peak amplitude observed was around 50% higher than that of the isolated cylinder case.

This phenomenon was then further explored and explained by Assi et al. in 2010, where it was categorised as a vortex influenced oscillation in which the magnitude

could keep on continuously increasing, even when f_s was much greater than f_o . The vortices of the leading body would provide a part of the oscillatory force for the system. This significant increase in force and amplitude is considered of immense potential for the present work.

2.4 Power Generation

The concept of power generation through VIVs has seen many different approaches and experiments. The main concept behind the energy generation has been the utilisation of the increased amplitude during lock in and conversion into useful energy. Several models have been proposed and explored through both analytical and numerical means. It is to be noted that the maximum efficiency obtainable in any generation will be limited to the Betz limit of extracting energy from flow.

Lefebure, Dellinger, François, & Mosé (2020) proposed a mechanical rig which uses the oscillation of a cylinder undergoing VIVs to drive a belt-generator system. The analytical model presented a theoretical efficiency of around 40%, with almost 2 MWh/m² of annual production with flow speeds beginning from 1 m/s. The model is presented below.

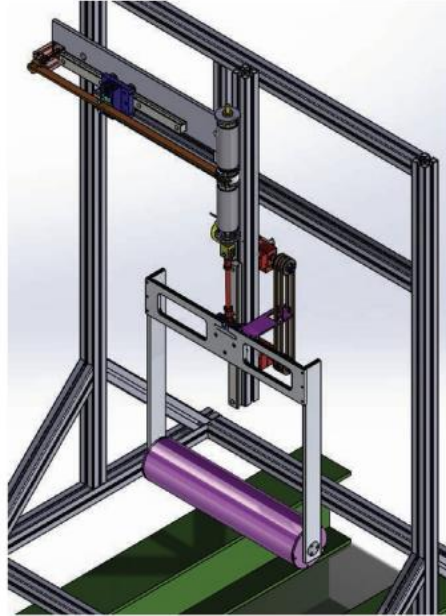


Figure 2: The model of Lefebure et. al., utilising a belt

Mehmood et. al. (2013) explored the possibility of a piezoelectric approach to power generation, with the piezoelectric element being simulated by the oscillation of the cylinder. The simulations evaluated results with the addition of the electromechanical damping and reached the conclusion that when the electrical load is variable, the greatest power generation lies somewhere in between the high and low values.

The most relevant work to the current undertaking is that of Soti, Thompson, Sheridan, & Bhardwaj (2017) which uses an electromagnetic coil and the principle of induction to demonstrate power generation in simulation. The effect of variable electromagnetic damping was analysed, and it was observed that the variable damping succeeded in

producing a larger peak power than a constant damping case. This result bodes well for the utilisation of this method to practically produce energy.

2.5 Existing Work

In the topic of energy generation through VIVs, perhaps the most influential operational work is the Vortex Induced Vibration Aquatic Clean Energy or VIVACE model. It uses the same principles discussed above and the gear-belt apparatus to generate energy from VIVs while installed on the seabed. VIVACE has seen success due to its scalability, modularity and flexibility. VIVACE is rated at an efficiency of 22%, and the amount of electricity generated can be scaled up indefinitely by joining together singular modules into larger plants.

The successful working of the VIVACE module presents an opening for the current undertaking to prepare an improved device to produce energy, utilising the basic concepts of VIVs and the energy generation techniques of electromagnetic induction.

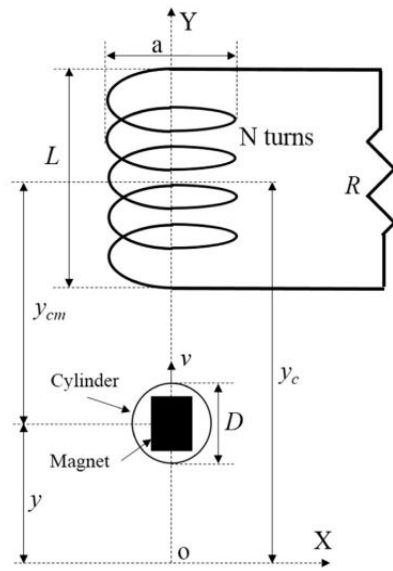


Figure 3: Electromagnetic generation set up from Soti et. al

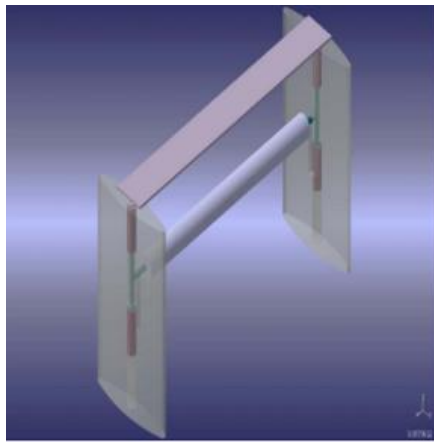


Figure 4: VIVACE Module

CHAPTER 3: METHODOLOGY

The objective in the section is to model and design a small device that will use VIVs to generate power. This will be split into three subsections: Numerical study of the flow, Experimental study of a prototype and Final Design.

3.1 Process Summary

The figure depicts a summary of the approach employed. The process was a top-down approach with iterative improvements.

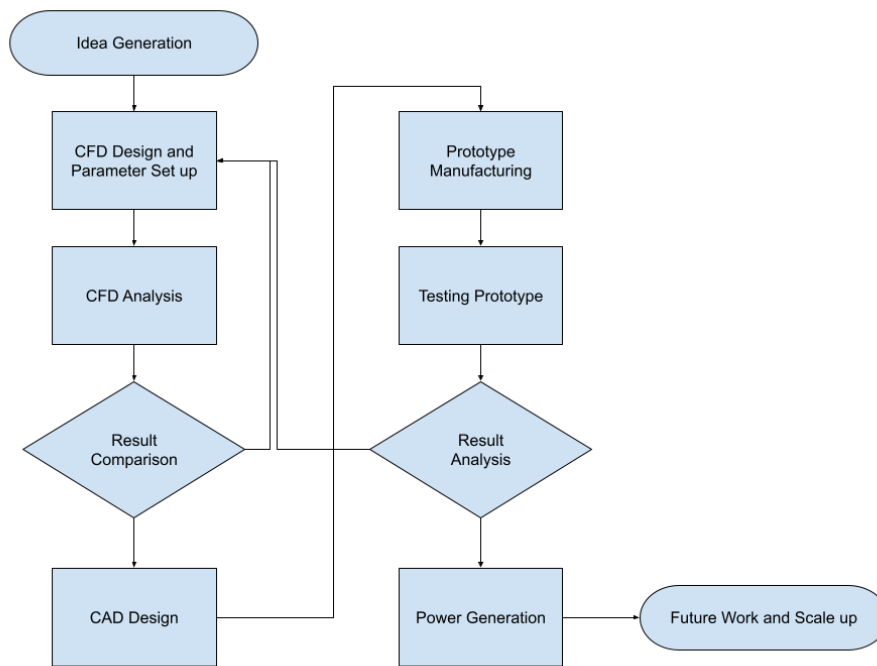


Figure 5: Process Flowchart

Commented [MA1]: @HASSAN MAJEED AKHUND
move the process summary here

Commented [MA2]: @HASSAN MAJEED AKHUND
move this proces summary thora ooper

3.2 Numerical Model

The objective of this study is to find the lock-in regime where resonance can occur. For this study RANS Shear-Stress-Transport (SST) k-w model will be used to predict the VIV phenomenon around circular cylinders at Re of 5000 and the low mass ratio of $m^* = 2.5$. ANSYS Fluent 19 is used for the study, k-w model is used along with dynamic meshing to evaluate. The study will be performed over a range of reduced velocities by changing the stiffness of the spring.

Following are some non-dimensional terms mentioned above

1. Reynolds number

This is defined as the ratio between viscous and inertial forces often the characteristic difference between turbulent and laminar flows.

2. Mass ratio

Mass ratio is defined as the ratio of bluff body's mass to the displaced fluid, it has a significant impact on the VIV phenomenon.

3. Reduced Velocity

This is a non-dimensional term to define velocity expressed by dividing the velocity by the diameter and the natural frequency.

The flow will be assumed incompressible as our application is meant mostly for water, which can be mathematically written as,

$$\frac{\partial u_i}{\partial x_i} = 0$$
$$\frac{\partial}{\partial t}(\rho u_i) + \frac{\partial}{\partial x_j}(\rho u_i u_j) = -\frac{\partial p}{\partial x_i} + \frac{\partial}{\partial x_j} \left(2\mu S_{ij} - \overline{\rho u_i u_j} \right)$$

where, ρ : time-average value of pressure

Commented [MA3]: turn all these equations to written text

u_i : time-average value of velocity

μ : molecular viscosity

S_{ij} : mean stress tensor, and

u_{ij} : Reynold's stress tensor

Further simplifying we obtain,

$$-\overline{\rho u_i' u_j'} = u_i \left(\frac{\partial u_i}{\partial x_j} + \frac{\partial u_j}{\partial x_i} \right) - \frac{2}{3} \left(\rho k + u_i \frac{\partial u_i}{\partial x_j} \right) \delta_{ij}$$

where, μ_i : eddy viscosity, a scalar characteristic, is often calculated from a transport variable

δ_{ij} : The Kronecker Delta, and

k : turbulent kinetic energy which is as follows

$$k = \frac{\overline{u_i' u_j'}}{2} = \frac{1}{2} (\overline{u^2} + \overline{v^2})$$

Pressure velocity coupled equations are solved using the SIMPLE algorithm as explained in the ANSYS manual (ref). Implicit first order method is used for unsteady terms while 2nd-order method is used for k-w transport equations also for momentum and convection equations. The first order upwind method is applied on diffusion terms.

The displacement of the Cylinder can be presented as (Guilmineau and Queutey),

$$\frac{d^2 Y}{d\tau^2} + \frac{4\pi z}{U_r} \frac{dY}{d\tau} + \frac{4\pi^2}{U_r^2} Y = \frac{2C_y}{\pi m^2}$$

where $Y = y/D$ denotes transverse displacement normalised by cylinder diameter

U_r : Reduced velocity,

z : structural damping ratio,

m : mass ratio, and

C_y : lift coefficient.

In the lock in region the vortex shedding frequency will approach the cylinder's natural frequency leading to resonance. The following equations can describe the behaviour:

$$y = A \sin(w_{ex}t)$$

$$C_y = C_L \sin(w_{ec}t + \phi)$$

$$C_{Lx} = C_L \sin \phi$$

$$C_{La} = -C_L \cos \phi$$

where w_{ex} is the oscillating frequency of the cylinder and C_L , C_{Lv} , and C_{La} are the lift coefficient, the velocity component of the lift and acceleration, respectively.

Amplitude ratio and frequency ratio can be defined as in Parkinson:

$$A^* = \frac{1}{4} \frac{C_{lv}}{\pi^3 m^* \zeta} \frac{f_n}{f_{ex}} \left(\frac{U}{f_n D} \right)^2$$

$$f^* = \left[1 + \frac{1}{2} \frac{C_{La}}{\pi^3 m^* A^*} \left(\frac{U}{f_n D} \right)^2 \right]^{\frac{1}{2}}$$

3.3 Flow Domain

The size of the domain and how the mesh or the grid is made has a significant impact on the study. It proves to be delicate balance between computational power, accuracy of the solution and stability of the solution. In literature quite a few different domain sizes have been used. Ranging from 16D by 30D (shao) while others have used sizes as small as 8D by 30D (Fang and Han). Due to the limited computational powers

Commented [MA4]: all of these equations to written text use mathpix or just write equations

smaller domain was chosen. After several iterations, a hybrid domain was selected with the triangular and quad elements.

The following figure shows the full flow domain:

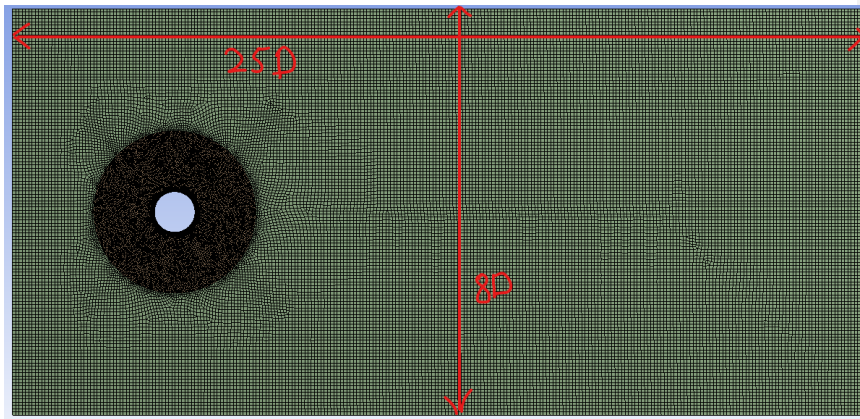


Figure 6: Full flow domain

This figure shows up close the near field triangular mesh and far field quad mesh. The tri mesh was chosen as only triangular mesh allows for dynamic meshing in ANSYS.

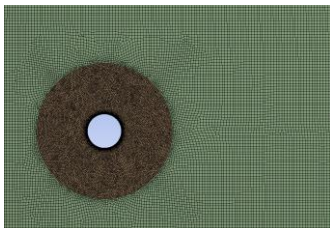


Figure 8: Near field triangular and far field quad mesh

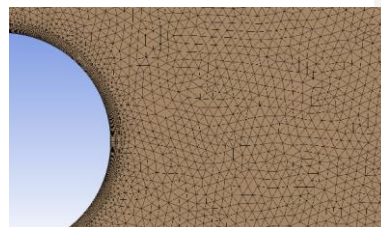


Figure 7: Inflation layer

The next figure shows a close-up of a fine inflation layer which was needed to define the boundary condition.

The following figures shows the flow domain for Cylinders in Tandem.

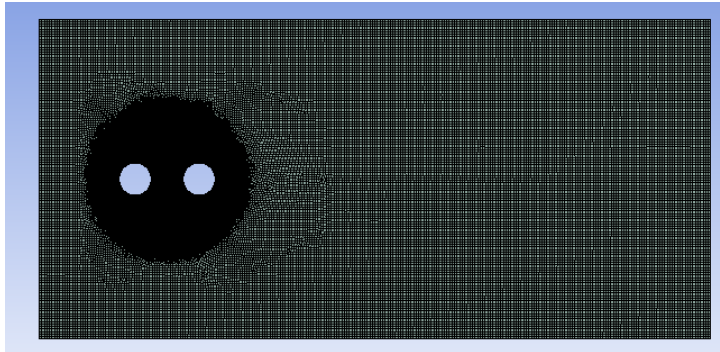


Figure 9: Mesh of the flow field for Cylinders in Tandem

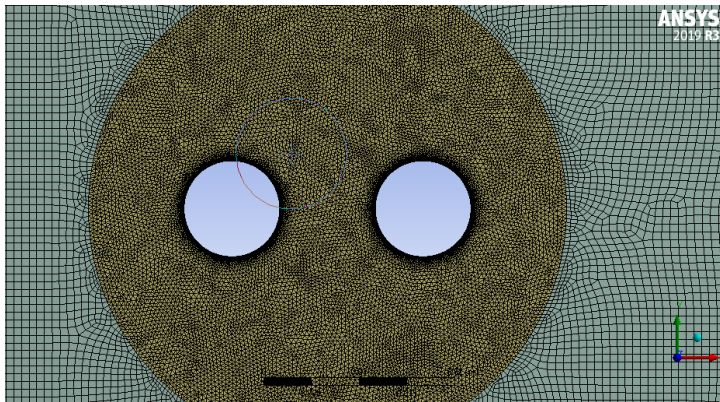


Figure 10: Mesh around the cylinders

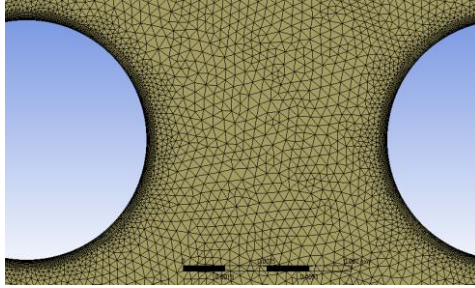


Figure 11: Close up of the tandem mesh

This mesh was made using the same ideas and thought process as for the single cylinder mesh, making sure the mesh was fine only where it was needed, and it was coarse everywhere else.

The same philosophy was followed while making meshes for the tandem cylinder, mesh was refined where a lot of motion was expected, it was kept coarse in the far regions. A very fine inflation layer was used to define the boundary conditions more accurately. The distance between cylinder boundaries and the first layer is particularly important especially since our vortex formation originates at the boundary layer. To resolve this a very fine inflation layer is used. The first layer thickness was determined using the $Y +$ value according the ANSYS manuals the $Y +$ should be less than or equal to 1 on the boundaries. The following figure shows a contour plot of $Y +$ value. Showing that the maximum value only goes up to around .931.



Figure 12: Contour plot of Y^+ value

A grid dependence study was carried out as well the following table shows the results for that. The literature value for C_d of smooth cylinder at 5000 Re comes out to .973. As seen in the table the grid T3 T4 T5 slowly approach that value. However, the grid T3 was used since the error was well within margin.

Table 1: Results of grid dependence study

	Cylinder Size	Near field size	Far field size	C_d (mean)
T1	250	8.00E-04	1.60E-03	1.04
T2	300	5.00E-04	1.00E-03	0.992
T3	400	4.00E-04	8.00E-04	0.979
T4	500	2.00E-04	4.00E-04	0.978
T5	600	1.00E-04	2.00E-04	0.975

3.4 Prototype Design

In view of the literature review it was evident that a comprehensive design methodology must be setup subjected to desired deliverables. Referring to the stated design problem, the oscillating cylinder energy harvester must generate electricity when placed in a stream of water flowing at $V_r \approx 4 - 10$ where the lock-in regime is noticed to exist. Not only is such a design easier to installed in already existing systems, the unconventional technology of oscillating cylinders aims to minimize the damage to marine wildlife while also minimizing the damage to subsea pipelines. The system can be used to generate renewable and consistent power near offshore oil rigs and continental telecom lines to provide auxiliary power.

3.4.1 Design Specification

In choosing our design, we determined the optimal parameters for our device to balance affordability, manufacturability and of course the most important aspect, which is performance. The design must fulfil certain requirements:

- Active energy harvesting mechanism
- Light weight assembly
- Efficient device to harvest flow energy from water

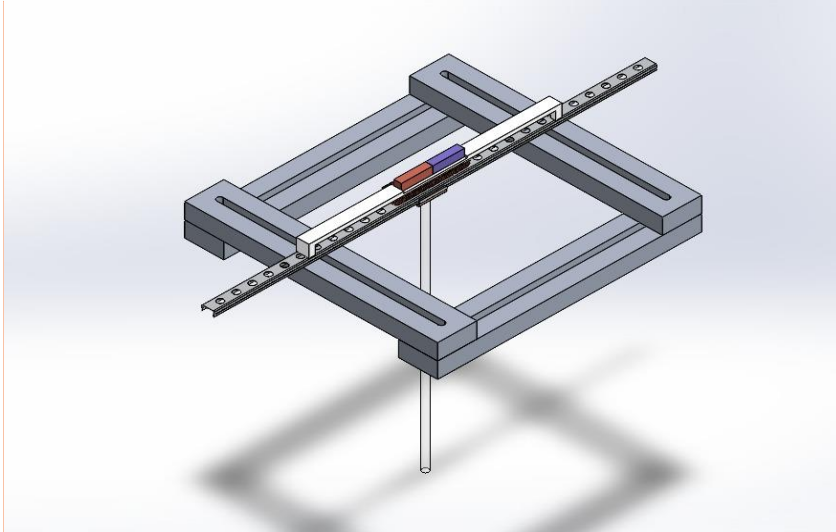


Figure 13: Initial Design

As indicated in the illustration, an early design was constructed. However, it was unsuitable to perform practical experimentation. The flow across the bluff body produces a force having two components, axial and lateral. For the design defined in our first prototype, it produced a significant error as the design was unable to overcome the axial forces and these forces led to the bearing locking on the slider due to the force produced in the axial direction.

Since the bearing ended up being locked, that resulted in extreme damping and the amplitude of the vibrations produced was inconsistent with the theoretically expected results.

Hence, the design was updated and is detailed in its final form in the following sections.

Commented [MA5]: @HAFIZ MUHAMMAD OSAMA KHAN new designs renders, @MUHAMMAD ABDULLAH HASSAN write the descriptions and why it was changed

3.4.2 Final design

The final design built up on the initial design with some improved features. The design is shown in figure 11.

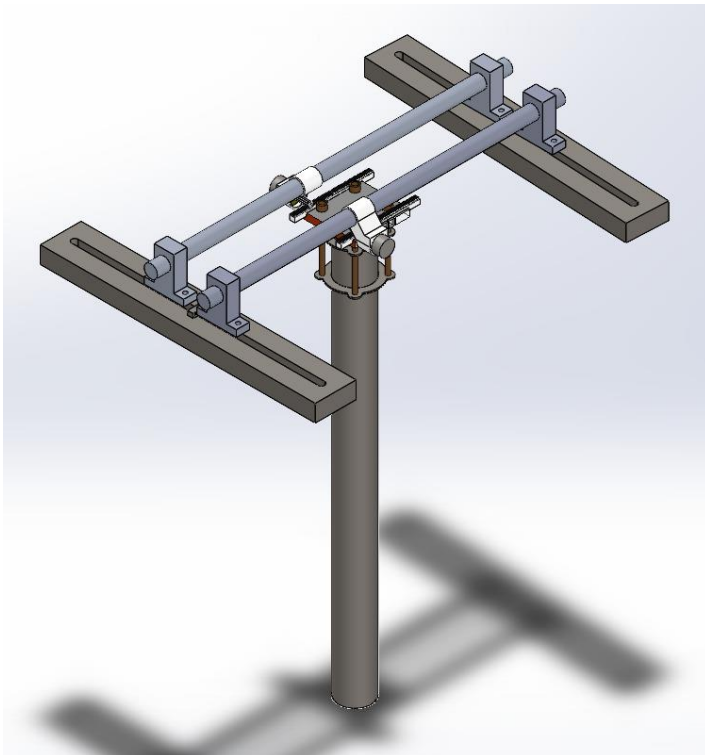


Figure 14: Final Design

The design prototype that was finalized has three main components:

- Bluff Body (Cylindrical Rod)
- Oscillatory Sub-Assembly
- Energy extraction system

The design also incorporates a stationary cylinder in line with the main cylinder. It is completely fixed at a variable distance upstream of the main cylinder to aid in wake induced vibration.

Harnessing the power from the oscillating cylinder was the most important consideration in the design. Since the oscillating movement is a linear movement, two main options to harness the energy was either to use a linear generator or to use a linkage which would transform the linear movement into rotary movement to drive a conventional generator. In this case, a conventional generator was driven by converting the linear motion through a rack and pinion assembly.

Bluff Body:

The bluff body consists of a rigid cylinder dipped in the flowing fluid. It experiences oscillations in the transverse direction due to the various phenomenon discussed above.

The properties required for the bluff bodies after consideration of the literature are as:

- Smooth surface (as surface roughness affects vortex shedding, so for the initial case a smooth cylinder would be desirable)
- Low mass ratio (for low inertial damping)

Keeping in mind these considerations, a stainless-steel pipe of diameter 50 mm was chosen. It was smoothed and it fell within the required mass ratio values. It was sealed to make sure that would be waterproof and impermeable, preventing any errors in results. This constituted the primary body. The secondary upstream cylinder was chosen to be a PVC pipe of a diameter of 65 mm. The secondary cylinder only serves

Commented [MAH6]: @MUHAMMAD SHAHZAIR ASIM is this right

as a device to generate vortices, meaning that there are no specific properties to ensure for.

Oscillatory Sub-Assembly:

The oscillatory system consists of the system on which the bluff body oscillates. Its main components are as follows:

- Rail
- Slider
- Linear bearing
- Returning springs

In the literature review most researchers had used pressurized air and electro-magnetic bearings to reduce friction, thus their friction was negligibly small. In our case procuring a system for either air bearings or magnetic bearings would cause a lot of problems. First, the issue would be budgeting. Second would be high quality/high precision machining required (preferably laser cutting) which would again increase the cost, not to mention that there is no laser cutting service provider available locally.

Although magnetic bearings are much easier to manufacture compared to air bearings due to no need of seals and fine machining, they pose another problem which is residual magnetism which needs to be removed after every few cycles, thus reducing the service life of the system.

At the end, a mechanical ball/roll bearing system was decided which is explained below. The initial design was to incorporate roller bearing in such a way that they can be used as wheels for free oscillations. But after market survey it was concluded that

such an approach while could be possible would result in a very complicated and heavy assembly which was counterintuitive to the purpose of this assembly (to provide ease in free oscillations).

The new and final design uses linear slide rail system inspired from the linear bearings used in CNC routers. After market research the following items have been finalized.

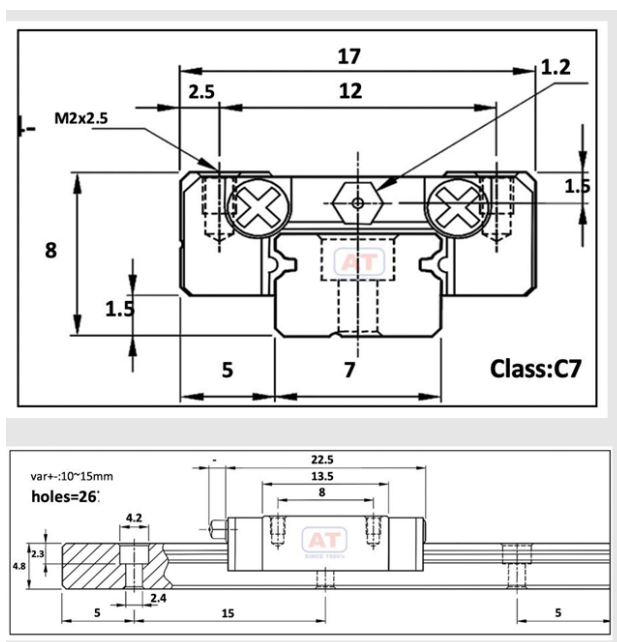


Figure 15: Linear slide rail schematic

The MGN series is a miniature rail slider series. The reason for choosing from the miniature series is that because now that the bluff body is very light, we do not need heavy duty equipment to uphold the weight.

The stiffness value of the returning springs was determined from CFD results and chosen to be 0.027 N/m. The springs are mounted onto the edges of the water tunnel frame and the linear slider.

Energy Extraction System:

For electrical energy extraction there are a few different methods that are available, including the use of piezo-electric flaps, electromagnetic induction through both linear displacement of a magnet and the more conventional generation using a generator. After debating the issue between the two types of induction, the conclusion reached was to utilise the generator setup, where the oscillation would be converted into rotary motion, which would be used to drive a generator. The mechanism for this is depicted in the diagram below

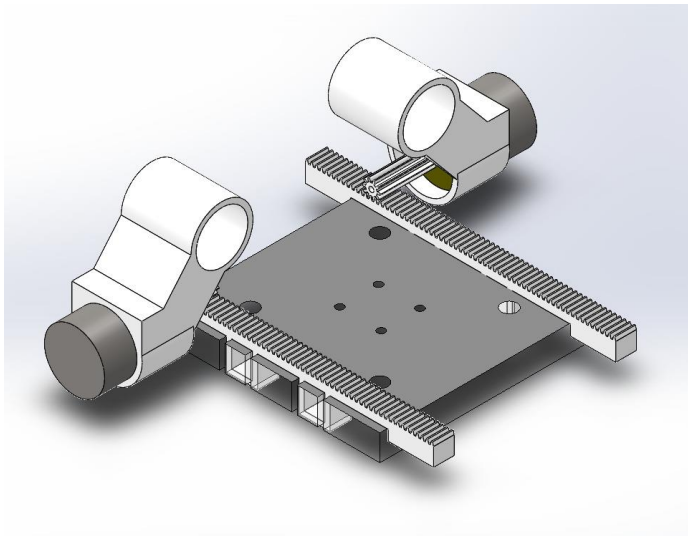


Figure 16: Energy Extraction Mechanism

Commented [MAH7]: @MUHAMMAD SHAHZAIR ASIM ye measure kar ke daal do

The mechanism uses a rack and pinion set up to utilise the oscillation in turning a motor. The motor can then begin to produce energy as oscillation occurs.

Commented [MAH8]: Kesay chalta hai ye boss
@MUHAMMAD SHAHZAIB ASIM @HAFIZ
MUHAMMAD OSAMA KHAN

CHAPTER 4: RESULTS AND DISCUSSION

4.1 Numerical Study Result for Single Cylinder

Simulations for the single cylinder were performed first to ascertain the accuracy of the set up. The figures showing the time history graphs of displacement of the cylinder plotted against time for specific Reduced velocities can be found in Appendix I. The following figures show a summary of the results. The results correspond well and the model in use is suitable for further simulation.

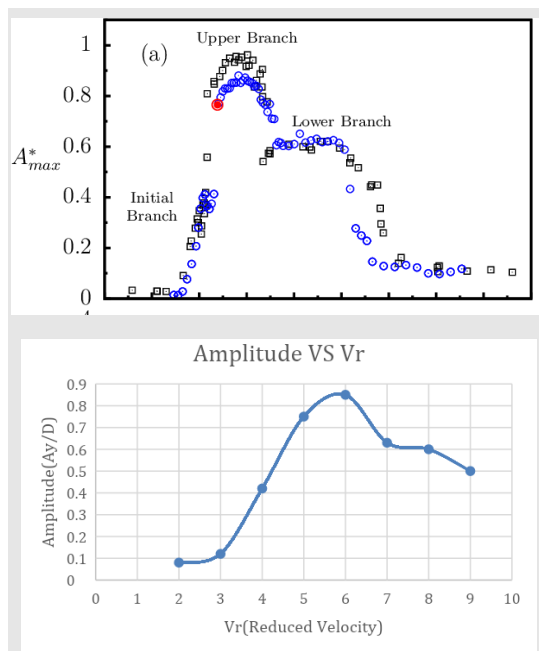


Figure 17: Amplitude vs Reduced Velocity for a Single Cylinder. Literature (top) vs. Current Results (bottom)

4.2 Numerical Simulation for Cylinders in Tandem

Following the evaluation and confirmation of the results for the single cylinder, simulations were performed on the double cylinder model. Appendix II has the entire time history graphs. A concise summary of the results is shown below.

Table 2: Amplitude of Oscillation at different reduced velocities and distances between cylinders

Reduced Velocity	Distance Between Cylinders in terms of diameter (50 mm)		
	1.5D	2D	3D
2	0.5D	0.3D	0.3D
4	0.6D	0.5D	0.4D
6	0.7D	0.5D	0.6D
8	0.9D	0.5D	0.6D

The graphical results are shown in comparison with the literature results are illustrated in Figure 14 on the next page. There is clear correlation in the trends of the current results and the results illustrated by Assi et. al.

Commented [MA9]: @HASSAN MAJEED AKHUND
need your Laptop to add all the, mesh diagrams weghaira

Commented [HMA10R9]: Ok le lena

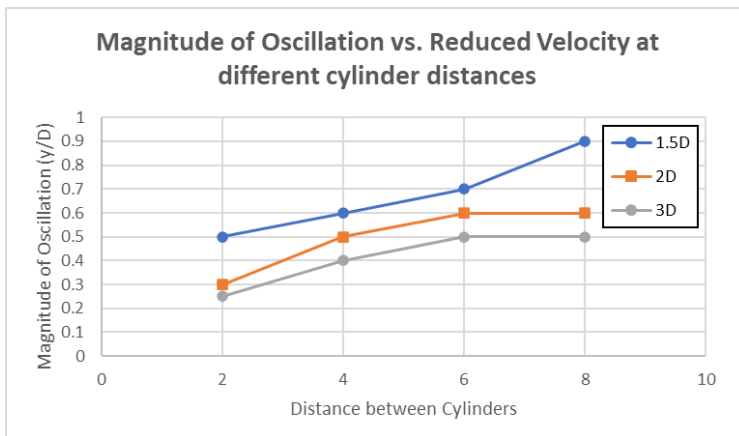
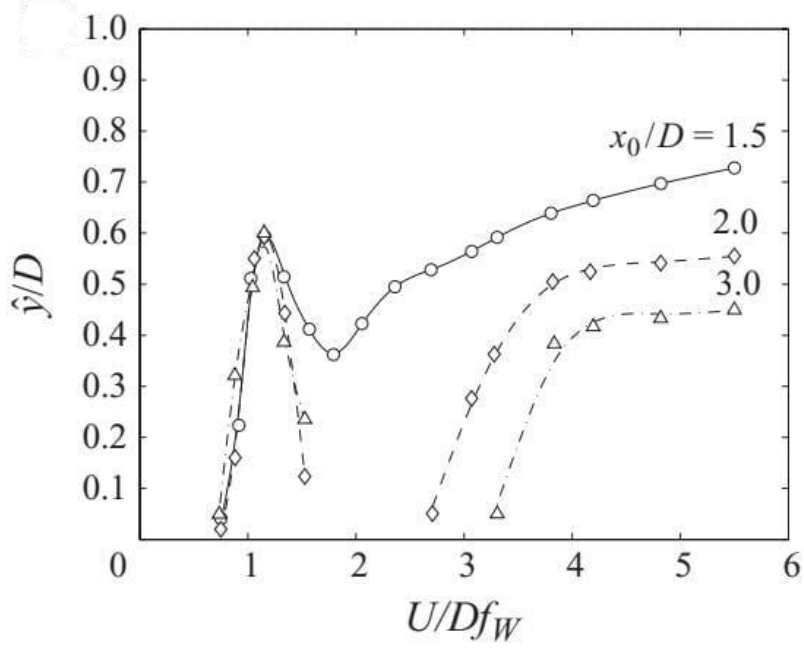


Figure 18: Oscillation magnitude vs Reduced Velocity, Assi et. Al. (top) and current results (bottom)

4.3 Displacement Results for Prototype

The prototype was used to run tests in the water tunnel available in NUST. The results are illustrated in the table and corresponding graph below.

Table 3: Amplitude of Oscillation at different flow speeds and distances between cylinders

Flow Speed (m/s)	Distance Between Cylinders in terms of diameter (50 mm)		
	1.5D	2D	2.5D
0.29	-	-	0.2D
0.30	0.5D	0.2D	-
0.31	-	-	0.3D
0.32	0.8D	-	-
0.33	-	-	0.5D
0.34	-	0.4D	-
0.35	-	-	0.6D
0.36	1.1D	-	-
0.37	-	0.7D	-

Commented [MA11]: @MUHAMMAD ABDULLAH HASSAN @HASSAN MAJEED AKHUND whoever has these, add a table then make a thora sa graph or compare it to the one form the literature.

Commented [MAH12R11]: Is doem

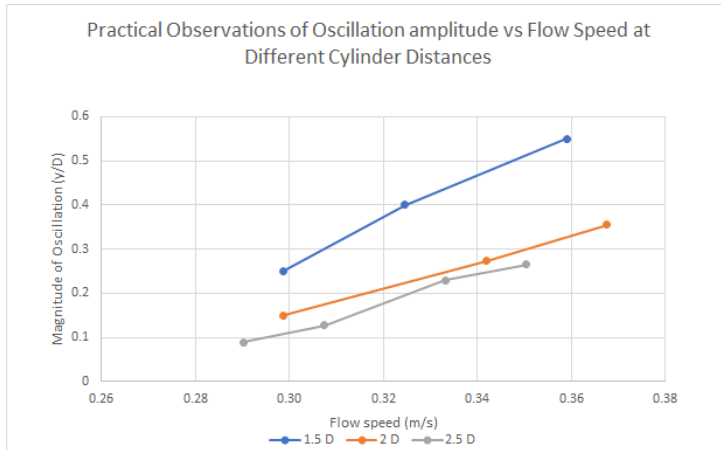


Figure 19: Practical Results of Oscillation Magnitude vs Flow Speed

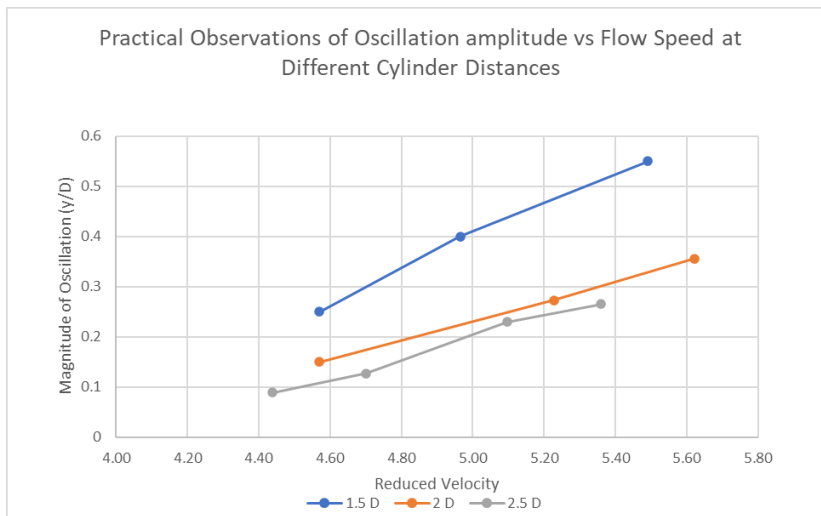


Figure 20: Practical results In terms of Reduced Velocity

For practical observations we were very limited by our testing capabilities, since we had a very low velocity water stream at our disposal, we could only get observations

for very low Reduced velocities. Taking all these results into account our practical observation are below both the literature work and the simulation predictions due to certain limitations.

After utilising the concept of cylinders in tandem the desired vibrations were observed. the vibrations amplitude observed compared to the simulated ones was a little less. This is mostly pertaining to a lot higher damping and friction in the actual model.

As the simulation was done under ideal conditions with the assumption that the axial force was negligible, the friction observed within the ball bearings were negligible therefore the vibrations produced theoretically were the maximum they could be, whereas in the practical case the vibrations produced were affected by the axial force as well as the friction within the bearings.

Beyond that we were very limited by our testing capabilities, as the water tunnel available to us was designed for low speed and low Reynolds numbers. Which meant a lot less power by the flow, but the same level of friction.

The results however showed that after considering all the losses. The amplitude was dampened by 30%

4.4 Power Generation Results

Every body of water that flows possesses kinetic energy due to its flow, it is our goal to extract as much as energy as we can from the flow as our setup allows, The vibrations due to vortex shedding produces oscillations of certain frequencies which at resonance maxes out and gives us the maximum amount of displacement possible.

Commented [MA13]: bro ye 30% kahan se aya just curious

Commented [HMA14R13]: You said 70% amplitudes based on theoretical could be harvested in practicality, so that implies 30% is lost

Commented [MA15R13]: okok

The oscillations produced by the flowing water is then harvested by the energy extraction in which a motor generates electricity by means of electromagnetic induction. The potential/efficiency that our system generates power is found by:

Extracted/available.

The displacement produced by the vibrations is used by the rack and pinion to transfer torque to the motors in the power extraction system. The motors then transfer the electrical power it generates to a rectifying bridge and then to a circuit containing a known resistor that serves as our load. The power thus extracted can be found by the simple formula $P = VI$ where V is the voltage observed by a DMM across the resistor and I is the current flowing through the circuit. It is to note that the power found from the formula is from a single motor.

Following were the results obtained by using a single motor to power.

Table 4: Electric Reading Results

Sr. No.	Resistance (Ω)	Voltage (V)	Current (mA)	Power (mW)
1	148	0.820	5.5	4.5
2	148	0.785	5.3	4.1
3	148	0.805	5.4	4.3

CHAPTER 5: CONCLUSION AND RECOMMENDATION

With the results obtained, and factoring in other variables, it can be recommended that the device is utilised for small scale use-cases, powered by small rivers or water channels. It can operate at a range of velocities, making it perfect for an application where the input can vary and the amount of energy available changes. The setup, once installed, also has little in the way of maintenance. If the installation is performed properly and all the components are properly sealed, it can keep running for a long duration without any intervention.

Regarding the physical aspects of the design itself it is easy to manufacture with a small number of parts. The prototype is sturdy, and it can withstand the conditions present in application where it may encounter debris in flow. The design is also sustainable with a small carbon footprint only at the time of manufacturing of parts.

Further research into the method and design is advised. There can be improvements made in both arrangement and in component selection. Regarding changes to the current design, a better bearing assembly could be an avenue of research, reducing the friction further. Several arrangements of the tandem cylinders can be investigated, with more cylinders and different configurations. The energy generation system may also behave differently if a direct induction method is used based upon that of magnets and copper wire coils instead of motors.

The design can also be altered from the onset, experimenting with a horizontal cylinder instead of a vertical one.

Commented [MA16]: @HASSAN MAJEED AKHUND like we discussed that day, ooper notes mein sab likha he just write it all here.
add some references to literature if it ever comes up

**APPENDIX I: TIME HISTORY GRAPHS OF DISPLACEMENT OF
SINGLE CYLINDER**

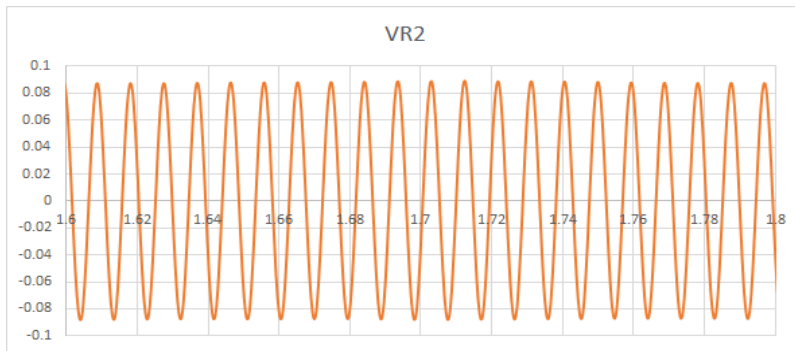


Figure 21: Displacement time history at V, 2

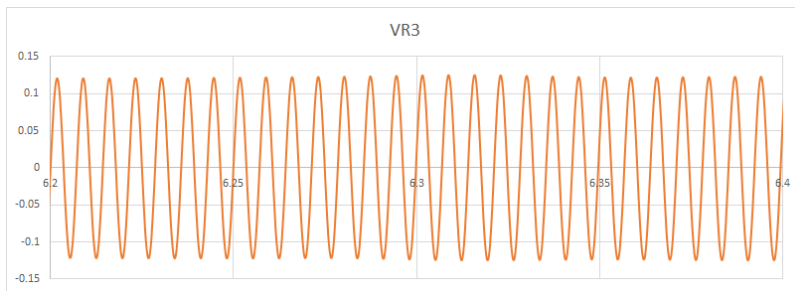


Figure 22: Displacement time history at V, 3

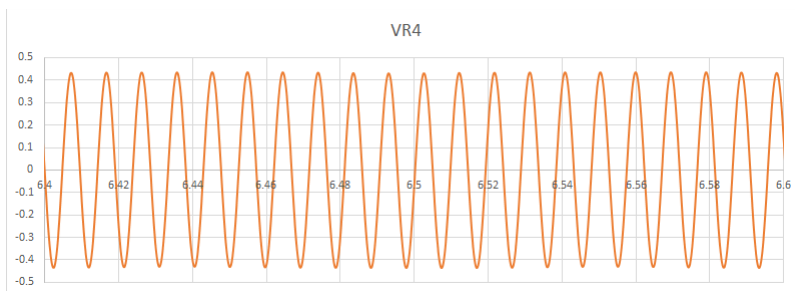


Figure 23: Displacement time history at V, 4

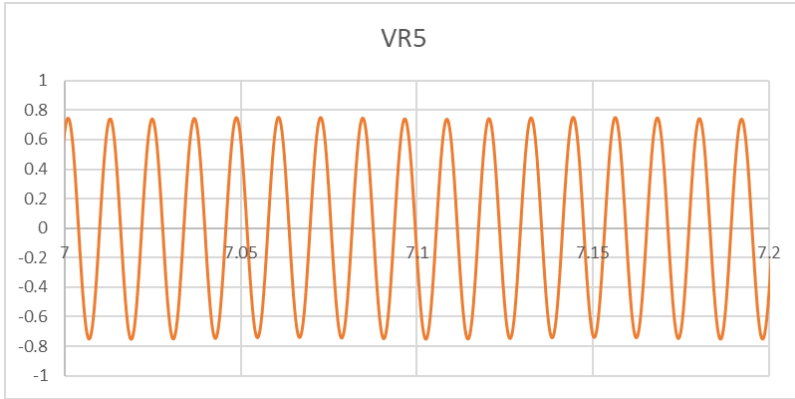


Figure 24: Displacement time history at V, 5

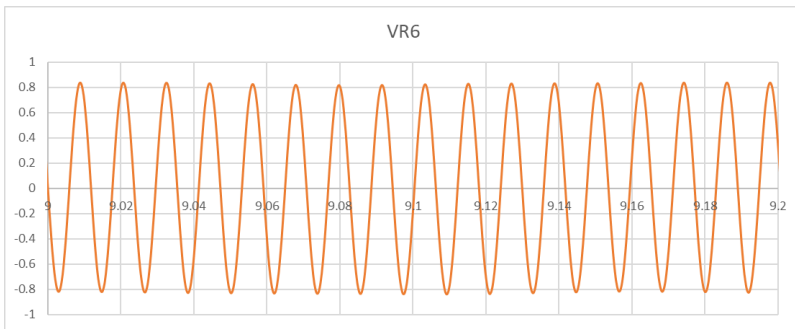


Figure 25: Displacement time history at V, 6

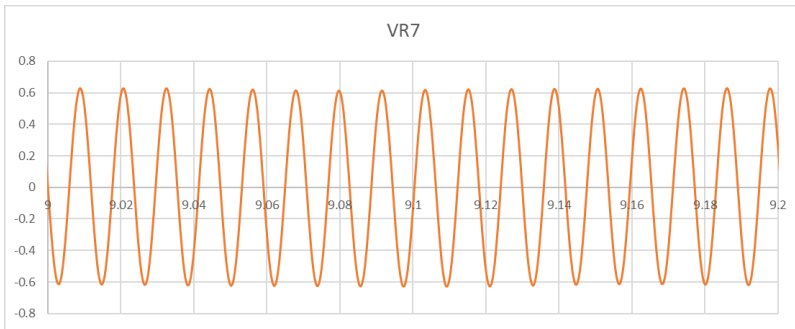


Figure 26: Displacement time history at V, 7

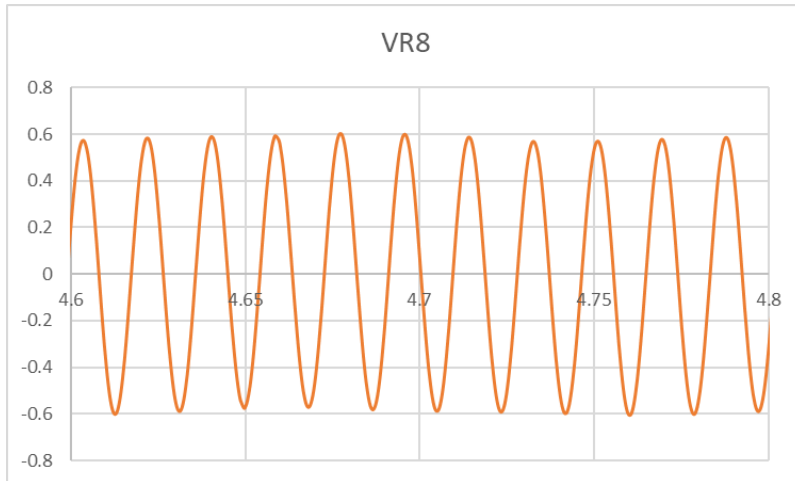


Figure 27: Displacement time history at V, 8

APPENDIX II: TIME HISTORY GRAPHS OF DISPLACEMENT
OF TANDEM CYLINDERS

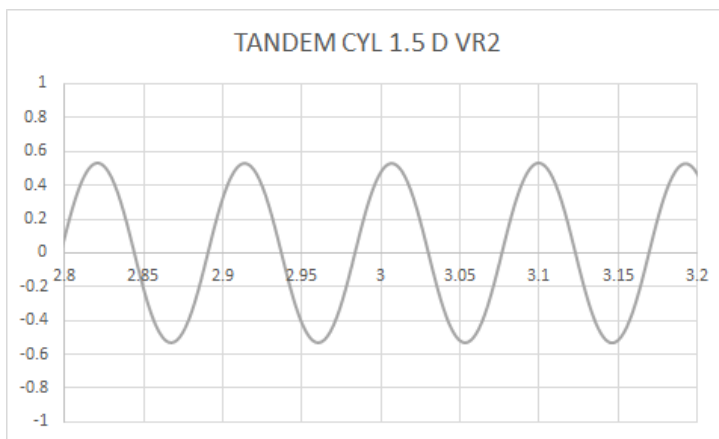


Figure 28: Displacement Time History at $V_r 2$ and in between distance 1.5D

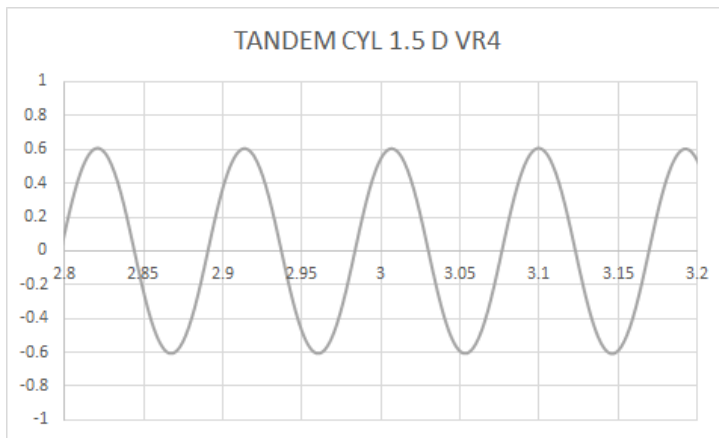


Figure 29: Displacement Time History at $V_r 4$ and in between distance 1.5D

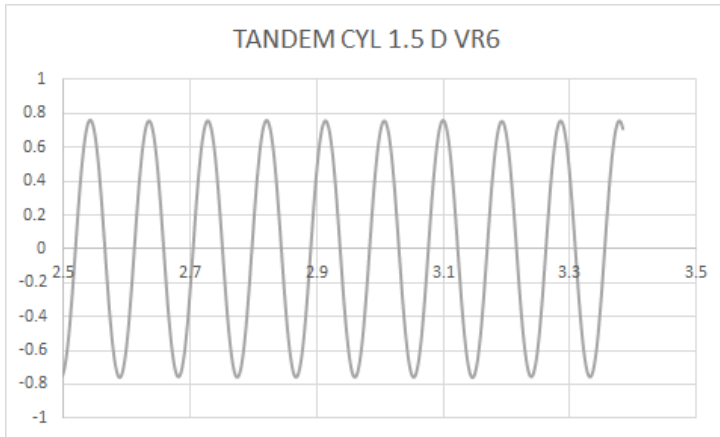


Figure 30: Displacement Time History at V_r 6 and in between distance 1.5D

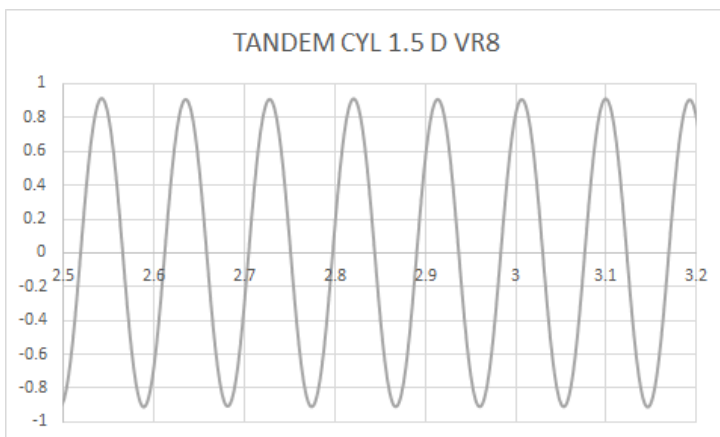


Figure 31: Displacement Time History at V_r 8 and in between distance 1.5D

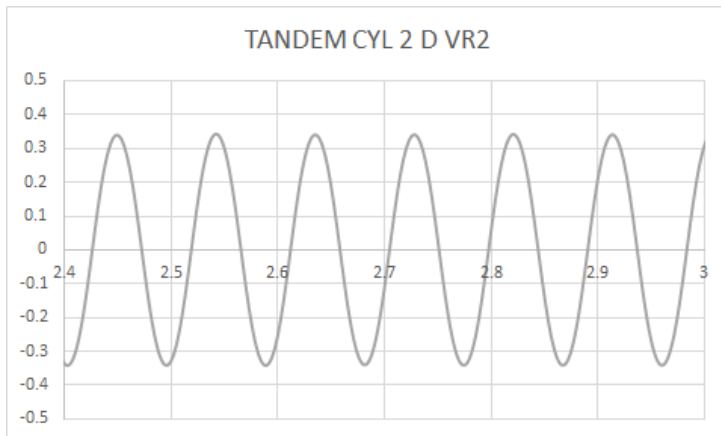


Figure 32: Displacement Time History at V, 2 and in between distance 2D

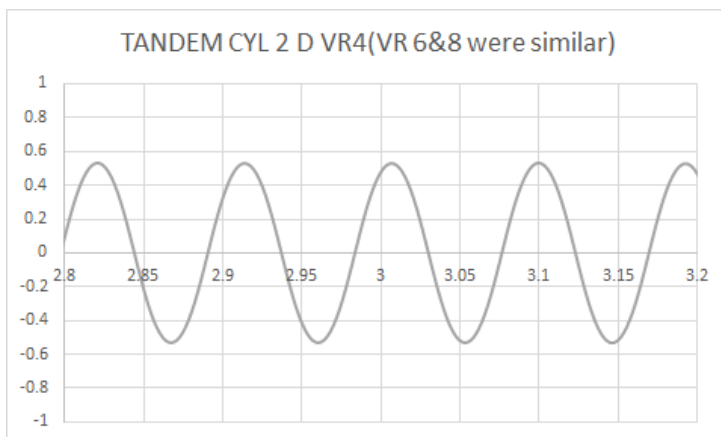


Figure 33: Displacement Time History at V, 4 and in between distance 2D

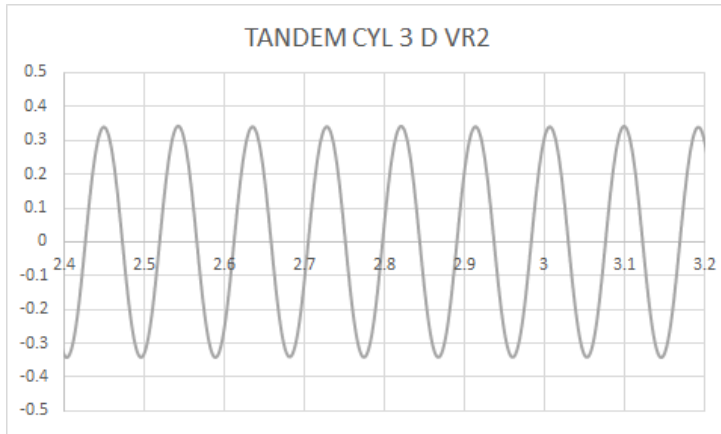


Figure 34: Displacement Time History at V, 2 and in between distance 3D

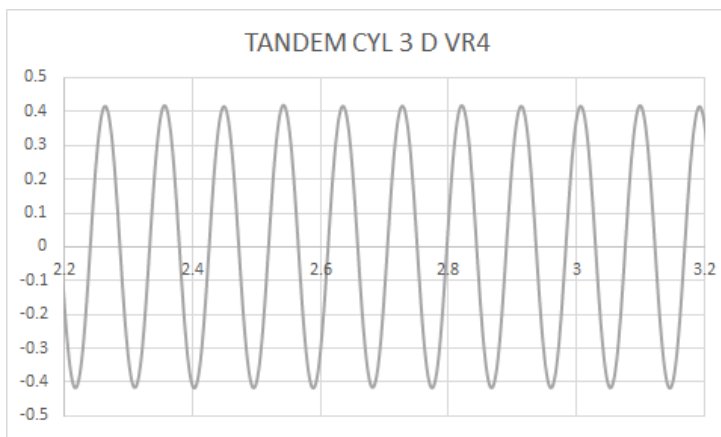


Figure 35: Displacement Time History at V, 4 and in between distance 3D

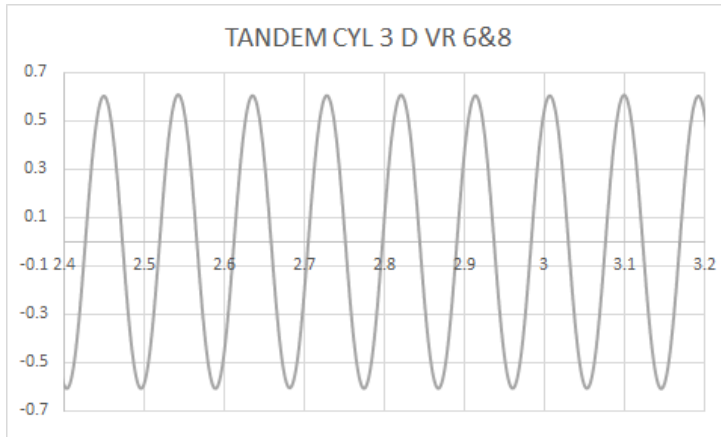


Figure 36: Displacement Time History at V, 6 and V, 8 and in between distance 3D

APPENDIX III: DRAWINGS OF COMPONENTS

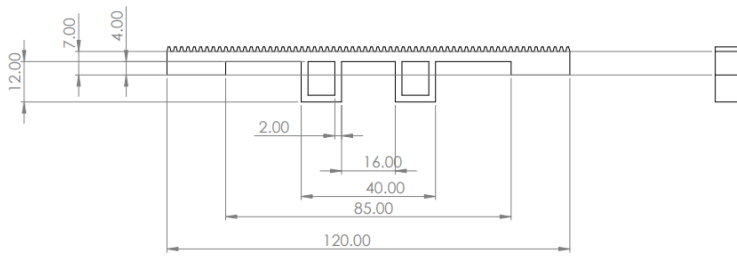


Figure 37: Drawing of Rack

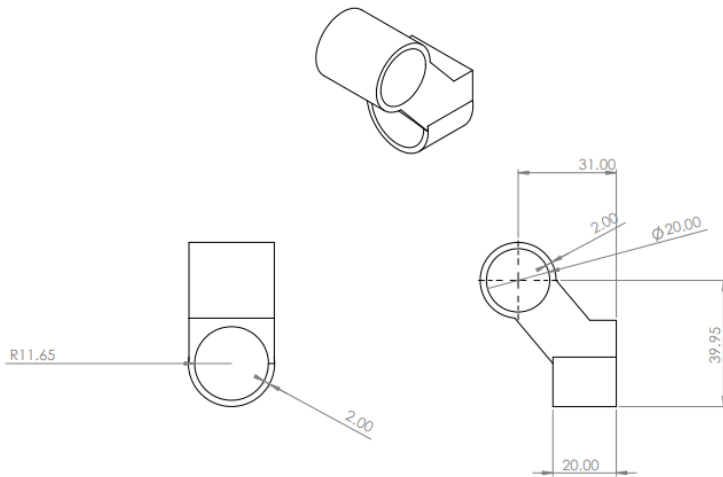


Figure 38: Drawing of Motor Holders

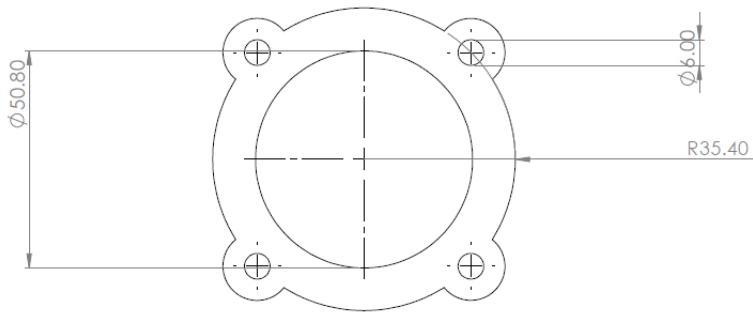


Figure 39: Drawing of Pipe Bracket

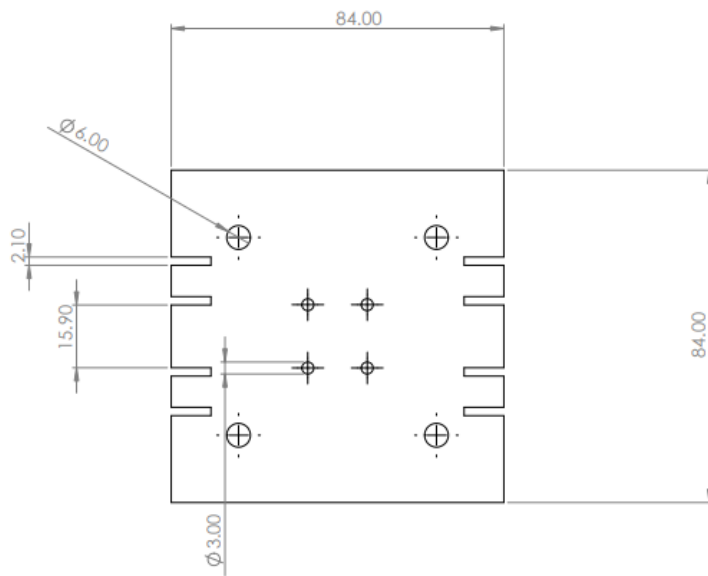


Figure 40: Drawing of Top Plate

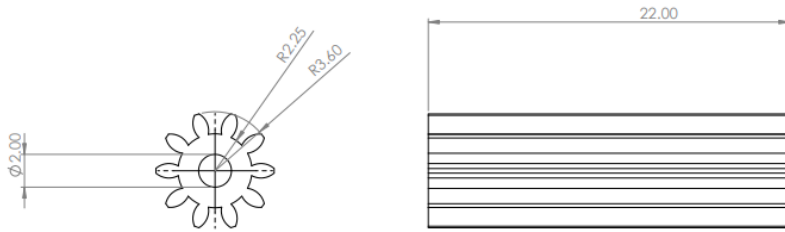


Figure 41: Drawing of Motor Gear

REFERENCES

- Bishop, R. E. D., & Hassan, A. Y. (1964). The lift and drag forces on a circular cylinder in a flowing fluid. *Proceedings of the Royal Society of London. Series A, Mathematical and Physical Sciences*, 277(1368), 32–50.
<https://doi.org/10.2307/2414647>
- Feng. (1968, January 1). The measurement of vortex induced effects in flow past stationary and oscillating circular and D-section cylinders. Retrieved from UBC Library Open Collections website:
<https://doi.library.ubc.ca/10.14288/1.0104049>
- Govardhan, R., & Williamson, C. H. K. (2000). Modes of vortex formation and frequency response of a freely vibrating cylinder. *Journal of Fluid Mechanics*, 420, 85–130. <https://doi.org/10.1017/s0022112000001233>
- Assi, G., Meneghini, J., Aranha, J., Bearman, P., & Casaprima, E. (2006). Experimental investigation of flow-induced vibration interference between two circular cylinders. *Journal of Fluids and Structures*, 22(6–7), 819–827.
<https://doi.org/10.1016/j.jfluidstructs.2006.04.013>
- Assi, G. R. S., Bearman, P. W., & Meneghini, J. R. (2010). On the wake-induced vibration of tandem circular cylinders: the vortex interaction excitation mechanism. *Journal of Fluid Mechanics*, 661, 365–401.
<https://doi.org/10.1017/s0022112010003095>
- Lefebure, D., Dellinger, N., François, P., & Mosé, R. (2020). Analytical and CFD study of the influence of control parameters on the maximum efficiency of a hydro-power conversion system based on vortex-induced vibrations. *Renewable*

Energy, 155, 369–377. <https://doi.org/10.1016/j.renene.2020.03.068>

- Mehmood, A., Abdelkefi, A., Hajj, M. R., Nayfeh, A. H., Akhtar, I., & Nuhait, A. O. (2013). Piezoelectric energy harvesting from vortex-induced vibrations of circular cylinder. *Journal of Sound and Vibration*, 332(19), 4656–4667. <https://doi.org/10.1016/j.jsv.2013.03.033>
- Soti, A. K., Thompson, M. C., Sheridan, J., & Bhardwaj, R. (2017). Harnessing electrical power from vortex-induced vibration of a circular cylinder. *Journal of Fluids and Structures*, 70, 360–373. <https://doi.org/10.1016/j.jfluidstructs.2017.02.009>
- Tofum, A., & Anand, N. M. (1985). Free span vibrations of submarine pipelines in steady flows—effect of free-stream turbulence on mean drag coefficients. *Journal of Energy Resources Technology*, 107(4), 415–420. <https://doi.org/10.1115/1.3231212>
- Williamson, C. H. K., & Roshko, A. (1988). Vortex formation in the wake of an oscillating cylinder. *Journal of Fluids and Structures*, 2(4), 355–381. [https://doi.org/10.1016/s0889-9746\(88\)90058-8](https://doi.org/10.1016/s0889-9746(88)90058-8)
- Guilmineau E, Queutey P. Numerical simulation of vortex-induced vibration of a circular cylinder with low mass-damping in a turbulent flow. *Journal of fluids and structures*. 2004; 19(4):449–66.
- Shao J, Zhang C. Numerical analysis of the flow around a circular cylinder using RANS and LES. *International Journal of Computational Fluid Dynamics*. 2006; 20(5):301–7
- Fang YY, Han ZL, editors. Numerical experimental research on the hydrodynamic

performance of flow around a three-dimensional circular cylinder. Applied Mechanics and Materials; 2011: Trans Tech Publ.